Experimental Investigation of Cooling Jets Mixing in a GasTurbine Cascade

G. Barigozzi*, F. Bassi, A. Perdichizzi*, M. Savini***
* Dip. di Ingegneria, Università di Bergamo, Viale Marconi 5, 24044 Dalmine (BG), Italy
Tel n. +39 035 277306 - Fax n. +39 035 562779 - Email perdi@unibg.it
** Dip. di Energetica, Università di Ancona, Via Brecce Bianche, 60100 Ancona, Italy

ABSTRACT

This paper presents an overview of the experimental results concerning a full coverage film cooled vane cascade investigation. Main objectives of this study were a detailed description of the cooling jets to mainstream aerodynamic mixing process and related loss generation mechanisms, together with the generation of a data set for CFD codes validation.

Experimental results have been obtained in a low speed wind tunnel for linear cascade testing. The tested blade profile is typical of a real gas turbine nozzle vane. Full coverage film cooling is achieved by means of 11 injection rows fed by a single internal cavity: 3 are located on the pressure side, 5 on the suction side and 3 in the leading edge region. All tests have been performed using air as coolant fluid, matching the design momentum flux ratio; this condition corresponds to an overall mass flow ratio equal to 2.5 %. A detailed experimental investigation has been performed in order to characterize the vane performances. Tests include mean and turbulent blade to blade velocity distributions, boundary layer profiles and a detailed description of cooling jet mixing process in the near hole region of the last pressure and suction side injection rows. Similar tests have been also performed on a solid blade cascade (without injection holes).

NOMENCLATURE

b	hole spacing, axial chord
$BR = (\rho_c u_c)/(\rho_e u_e)$	blowing ratio
c	blade chord
D	hole diameter
g	pitch, mass flow rate
h	blade height, enthalpy
$H_{12} = \delta^*/\theta$	shape factor
$I = (\rho_c u_c^2)/(\rho_e u_e^2)$	momentum flux ratio
M	Mach number
p	pressure
$\mathrm{Re}_{2is} = U_{2is} c/\nu$	isentropic outlet Reynolds number
$\mathrm{Re}_\theta = U_e \theta/\nu$	momentum thickness Reynolds number
s, n, h	local coordinate system
$Tu = \sqrt{0.5(\overline{u'^2} + \overline{v'^2})}\,/\,U_{2is}$	turbulence intensity, %
u, v	velocity components
U_e	local free-stream velocity
x	axial coordinate
β	flow angle, with respect to tangential direction
δ^*	displacement thickness

Paper presented at the RTO AVT Symposium on "Advanced Flow Management: Part B – Heat Transfer and Cooling in Propulsion and Power Systems", held in Loen, Norway, 7-11 May 2001, and published in RTO-MP-069(I).

Report Documentation Page

Form Approved
OMB No. 0704-0188

1. REPORT DATE	2. REPORT TYPE	3. DATES COVERED
00 MAR 2003	**N/A**	**-**

4. TITLE AND SUBTITLE	5a. CONTRACT NUMBER
Experimental Investigation of Cooling Jets Mixing in a Gas Turbine Cascade	5b. GRANT NUMBER
	5c. PROGRAM ELEMENT NUMBER
6. AUTHOR(S)	5d. PROJECT NUMBER
	5e. TASK NUMBER
	5f. WORK UNIT NUMBER
7. PERFORMING ORGANIZATION NAME(S) AND ADDRESS(ES) **NATO Research and Technology Organisation BP 25, 7 Rue Ancelle, F-92201 Neuilly-Sue-Seine Cedex, France**	8. PERFORMING ORGANIZATION REPORT NUMBER
9. SPONSORING/MONITORING AGENCY NAME(S) AND ADDRESS(ES)	10. SPONSOR/MONITOR'S ACRONYM(S)
	11. SPONSOR/MONITOR'S REPORT NUMBER(S)

12. DISTRIBUTION/AVAILABILITY STATEMENT
Approved for public release, distribution unlimited

13. SUPPLEMENTARY NOTES
Also see ADM001490, presented at RTO Applied Vehicle Technology Panel (AVT)Symposium held in Leon, Norway on 7-11 May 2001, The original document contains color images.

14. ABSTRACT

15. SUBJECT TERMS

16. SECURITY CLASSIFICATION OF:			17. LIMITATION OF ABSTRACT	18. NUMBER OF PAGES	19a. NAME OF RESPONSIBLE PERSON
a. REPORT **unclassified**	b. ABSTRACT **unclassified**	c. THIS PAGE **unclassified**	**UU**	**14**	

γ	specific heat ratio
θ	momentum thickness
ρ	flow density
ζ	energy loss coefficient

Subscripts

1	inlet
2	exit
c	cooling flow
e	main flow
is	isentropic
t	total

Superscripts

$\bar{}$	mean
'	fluctuation

INTRODUCTION

Full coverage film cooling is the way commonly employed in modern gas turbines to get higher turbine inlet temperatures. Coolant injection strongly affects the profile performance and for this reason its influence on heat transfer and loss production has been extensively investigated during the last years. The goal is to improve the injection modes in order to get higher effectiveness with minimum coolant consumption.

Coolant injection influence on cascade performance is generally evaluated on the basis of mixed out 2D loss coefficient distributions (Urban et al. [1]), taking into account all sources of loss, i.e. coolant jet to mainstream mixing, profile boundary layer development and downstream mixing. In order to evaluate each contribution to the overall loss production, downstream 2D loss distributions are measured and boundary layer losses are computed using theoretical prediction methods (e.g. Hartsel [2]); downstream mixing losses are then obtained by difference.

Recently, Reynolds-Averaged Navier-Stokes (RANS) solvers, which directly compute all the flow field (Walters and Leylek [3], Bassi et al. [4]), have been replacing theoretical prediction methods. The predictive capability of RANS solvers heavily depends on numerical accuracy and turbulence modelling reliability. This means that RANS solutions need to be carefully validated against accurate experimental data. For this purpose downstream measurements do not suffice and further detailed experimental data concerning the boundary layer development and the near hole flow field are needed. Obviously, such an investigation is useful in itself to gain more insight into the loss generation mechanisms.

Detailed flowfield measurements in the near hole region of a large scale cascade with showerhead injection are reported by Ardey and Fottner [5], while Brandt et al. [6] report on 3D hot wire measurements in the near hole region of a large scale turbine blade with suction side cooling through a single row of cylindrical holes. Barigozzi et al. [7] have documented a boundary layer investigation aimed at studying the influence of coolant injection on boundary layer development and loss generation along the pressure and suction side rear part of a full coverage film cooled vane. They find that the jet effects vanish quite rapidly and that showerhead injection induces transition along the suction side, while the pressure side boundary layer has been found to remain laminar up to the trailing edge.

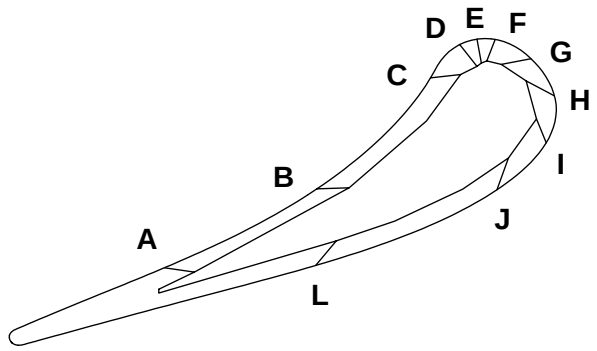

Figure 1: Cooled vane and injection hole locations.

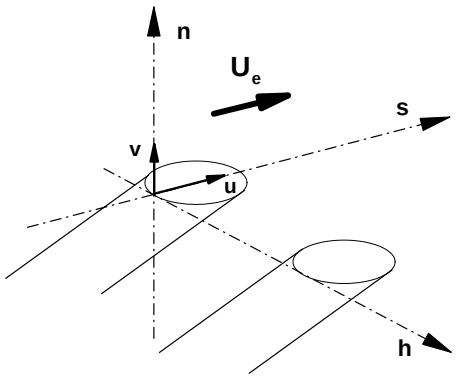

Figure 2: Hole coordinate system.

Table 1:

Cascade geometry	**Operating conditions**
g/c = 0.86	β_1 = 90°
h/c = 1.04	M_1 = 0.06
β'_2 = 21°	M_{2is} = 0.2
c = 133.7 mm	Re_{2is} = 0.66 10^6
no. of blades = 7	Tu = 1.7 %

Table 2: Cooling system characteristics

g_c/g_e	0.025			
	Pressure side		**Suction side**	
$g_c/g_{c,tot}$	0.363		0.637	
	A	B	J	L
x/b	0.75	0.49	0.49	0.74
B/D	3.125	3.125	2.7	4.5
α	35°	35°	35°	35°
BR	1.1	1.86	0.71	0.79

Starting from these results, a detailed LDV investigation of the flow field in the near hole region of the last pressure and suction side injection rows has been carried out. In order to get significant measurements, the cascade vanes have been tested in a low turbulence, low Mach and Reynolds number flow. In the following section the experimental set-up and the measurement technique are described. The section of results presents a comprehensive set of experimental data concerning: mean flow field, near wake region, boundary layer development, overall cascade performance and near hole region. In the last section some conclusions are given.

EXPERIMENTAL SETUP AND TESTING CONDITIONS

The tests were performed in the low-speed wind tunnel for linear cascades of the Thermo-Fluid Dynamic Laboratory of Bergamo University. The tunnel is a continuous running suction type facility, which is completely Plexiglas made to allow free optical access. Details of the facility, including the secondary air supplying system, are reported in Barigozzi et al. [7]. The cascade consists of 7 vanes typical for a first stage of an industrial gas turbine. The only difference is that trailing edge ejection has not been performed, due to manufacturing constraints. The tested vane and hole locations are presented in Figure 1. A single internal cavity in the film cooled airfoil feeds 11 rows of cylindrical holes (D = 0.7 mm) distributed along the profile, thus assuring the full

coverage film cooling. The showerhead region has 3 rows of holes, while 5 rows are on the suction side and 3 on the pressure side. Three film cooled blades made of epoxy resin have been manufactured, thus giving identical coolant injection on the two central passages.

A set of solid vanes, i.e. with no injection holes, has also been tested. Two adjacent vanes have been instrumented, with 25 and 20 pressure taps, respectively on suction and pressure sides, to get profile static pressure distribution at mid-span. Cascade geometry and operating conditions are given in Table 1. Notwithstanding that the operating conditions of this stage nozzle vane are in the high subsonic regime (M_{2is} = 0.85), tests were done at low speed, with an outlet Mach number M_{2is} = 0.2. This in order to make the blade boundary layer thickness large enough to get significant measurements in the film cooling region. Of course, the resulting pressure distribution along the blade is different from design conditions, causing two main effects. The first one is the presence of lower pressure gradients which cause a different boundary layer development. The second aspect is a different share of coolant flow among injection rows. Due to the presence of a single internal cavity, the coolant flow distribution is affected by changes in the profile pressure distribution. In particular, lower blowing rates will occur on the suction side. The variation of blowing ratio of individual rows has been estimated to be not too large. All tests have been performed at a Reynolds number equal to half the design value and at a low inlet turbulence intensity level Tu = 1.7 %, measured half a chord upstream of cascade inlet. The Reynolds number and also, as reported by Camci and Arts [8], the turbulence intensity level are expected to have a small influence on the cooled vane performance, as suction side boundary layer transition is triggered by showerhead injection.

Total pressure and temperature of injected flow are measured in the blade cavity by means of pressure taps and T type thermocouples. Following the procedure described by Dossena et al. [9], coolant share among injection rows has been evaluated on the basis of discharge coefficients, allowing the definition of blowing and momentum flux ratio for each row of holes. Table 2 resumes the main characteristics of coolant flow for the last two rows on both pressure (A and B) and suction (J and L) sides, where the boundary layer and near hole investigations have been carried out. Osnaghi et al. [10] have shown that results at different density ratios are well correlated using the momentum flux ratio. Air at ambient temperature was blown as coolant flow, with an overall mass flow ratio of 2.5 %, corresponding to the design momentum flux ratio, thus assuring similar mass averaged losses.

Measurement technique and testing procedure

A four beam, two color LDV system (DANTEC Fiber Flow) has been used. For the near hole investigation, a 140 mm focal length front lens produces a measurement volume of 0.04 mm in diameter and 0.3 mm in length. In all the other cases, i.e. for boundary layer and near wake investigations, a 200 mm focal length front lens has been used, giving rise to a measurement volume of 0.06 mm diameter and 0.6 mm length. Anyway, the measurement volume is located inside the test section so that its larger dimension is aligned with the spanwise direction. Sawdust smoke has been used to seed both main and cooling flows independently. Mean and fluctuating velocity components have been corrected for velocity bias (Boutier [11]). Based on a 95 % confidence level, statistical uncertainties for mean and RMS velocities of 1.24 % and 4.4 %, respectively, have been obtained considering 1000 collected data and a turbulence intensity level of 20 %. BSA processor accuracy can be estimated to be lower than 1 % (Modarres et al. [12]). A computer controlled three axis traversing system driven by stepping motors assures a probe minimum linear displacement of 10 μm. The probe can also be continuously rotated around all three axis, thus making it possible to approach the blade surface everywhere.

The boundary layer behavior in the region corresponding to the last two rows on both pressure and suction side and the near wake region have been previously investigated (Barigozzi et al. [7]) with

the same technique. A miniaturized 5-hole pressure probe (1.8 mm head) has been also traversed downstream of the cascade; 6 traverses have been performed, from *x/b* = 0.13 up to *x/b* = 0.55 downstream of the trailing edge. Uncertainties have been estimated to be 0.15 % of dynamic pressure. These data have been used to compute energy loss coefficient distributions along the vane surface and in the downstream region.

In the near hole investigation, the domain includes the near hole region of last injection row A on pressure side and L on suction side. This region has been investigated performing 2D measurements on a 3D grid. Figure 2 presents the vane geometry with injection locations while Figure 3 shows the coordinate system centered on the hole centerline leading edge. The grid consists of 10 measurement planes *(h, n)*, starting 1 mm upstream of rows A and L. Plane spacing in *s*-direction is initially set to 1 mm close to the row, and then increased to 2 mm going further downstream. Each plane is divided into 11 spanwise traverses of 10 points each one, thus covering one hole pitch with an overall of 1100 measurement points. Traverse spacing has been increased close to injection location and approaching the blade surface, where the first traverse has been performed at *n* = 0.2 mm for row A and 0.35 mm for row L. In each measurement point, mean and RMS velocity components lying in the *(s, n)* plane have been acquired in coincidence mode, with data rates ranging from 0.1 up to 6 kHz going far from the wall.

RESULTS

Mean flow field

Figures 3 and 4 present the profile isentropic Mach number and the Mach number isolines in the blade to blade plane located at mid span. These data have been obtained testing the solid vane cascade. Both Figures show the presence of a continuous flow acceleration on the blade pressure side up to the trailing edge, while the suction side is characterized by a strong initial acceleration followed by a moderate diffusion. There is no evidence of flow separation, and the flow field displays a good periodicity.

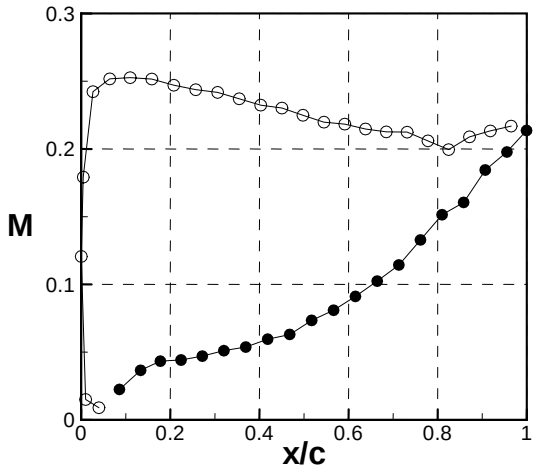

Figure 3: Profile isentropic Mach number.

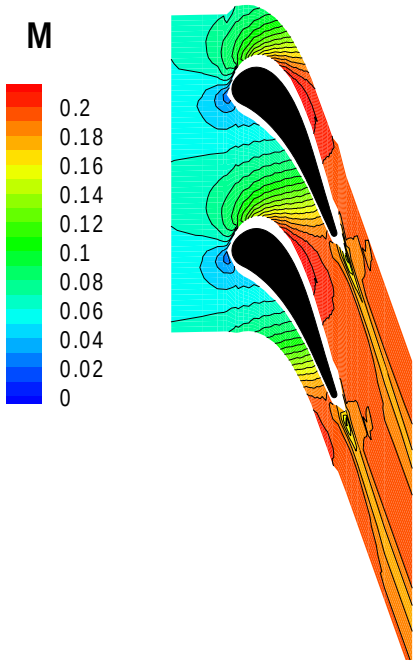

Figure 4: Blade to blade Mach number distribution.

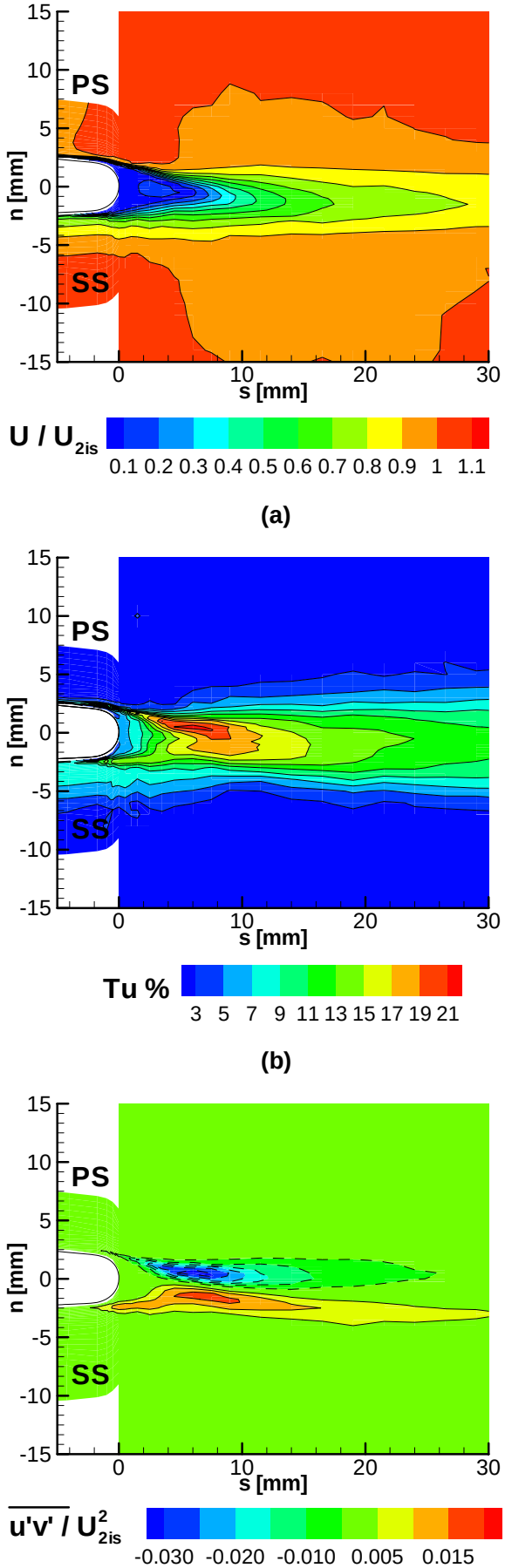

Figure 5: The near wake flow field

The near wake region

Mean velocity, turbulence intensity and $\overline{u'v'}$ component distributions in the near wake region are presented in Figure 5. Note that *Tu* and $\overline{u'v'}$ are not pure turbulent quantities because they also include the mean flow unsteadiness due to vortex shedding. All quantities are normalized using the outlet isentropic velocity $U_{2,is}$, based on the downstream wall static pressure at $x/c = 0.5$ and inlet total conditions. The mean flow velocity distribution (Figure 5(a)) puts in evidence the difference between the thin boundary layer along the pressure side and the thicker boundary layer that develops along the suction side. Also the *Tu* distribution (Figure 5(b)) on the trailing edge sides is rather different and the higher value of the pressure side peak can be attributed to a stronger vortex shedding activity. The shear stress $\overline{u'v'}$ (Figure 5(c)) shows a typical two-core distribution, with the sign changing across wake centerline.

The boundary layer investigation

A detailed boundary layer investigation has been performed along both pressure and suction side rear parts, including the two last injection rows (A and B on the pressure side and J and L on the suction side). These data have been already reported and thoroughly discussed by Barigozzi et al. [7]. Here only the traverses closest to the trailing edge on both pressure (Figure 6(a)) and suction (Figure 6(b)) side are presented. Coolant injection along the pressure side does not alter the boundary layer behavior, that remains laminar up to the trailing edge, as the high acceleration prevents transition. On the contrary, showerhead injection induces boundary layer transition along the suction side, and the fully turbulent boundary layer along the whole investigated region, becomes 4.3 mm thick close to the trailing edge. Note that, in the solid vane case, the boundary layer was found to be laminar at the location corresponding to injection row J.

Starting from boundary layer traverses, integral parameters have been computed. Figure 7 presents the integral parameters (displacement

thickness, shape factor and momentum thickness Reynolds number) on the boundary layers developing along the vane pressure (Figure 7(a)) and suction (Figure 7(b)) sides. These results confirm the laminar character of the pressure side boundary layer, while the suction side boundary layer is fully turbulent up to the trailing edge, without any evidence of separation.

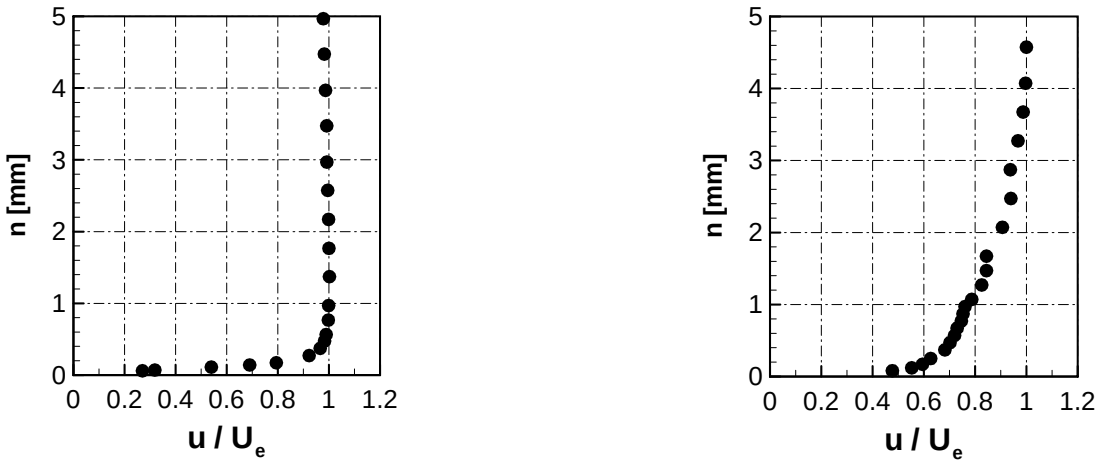

(a) Pressure side (x/c = 0.95)

(b) Suction side (x/c = 0.98)

Figure 6: Boundary layer profiles close to the trailing edge.

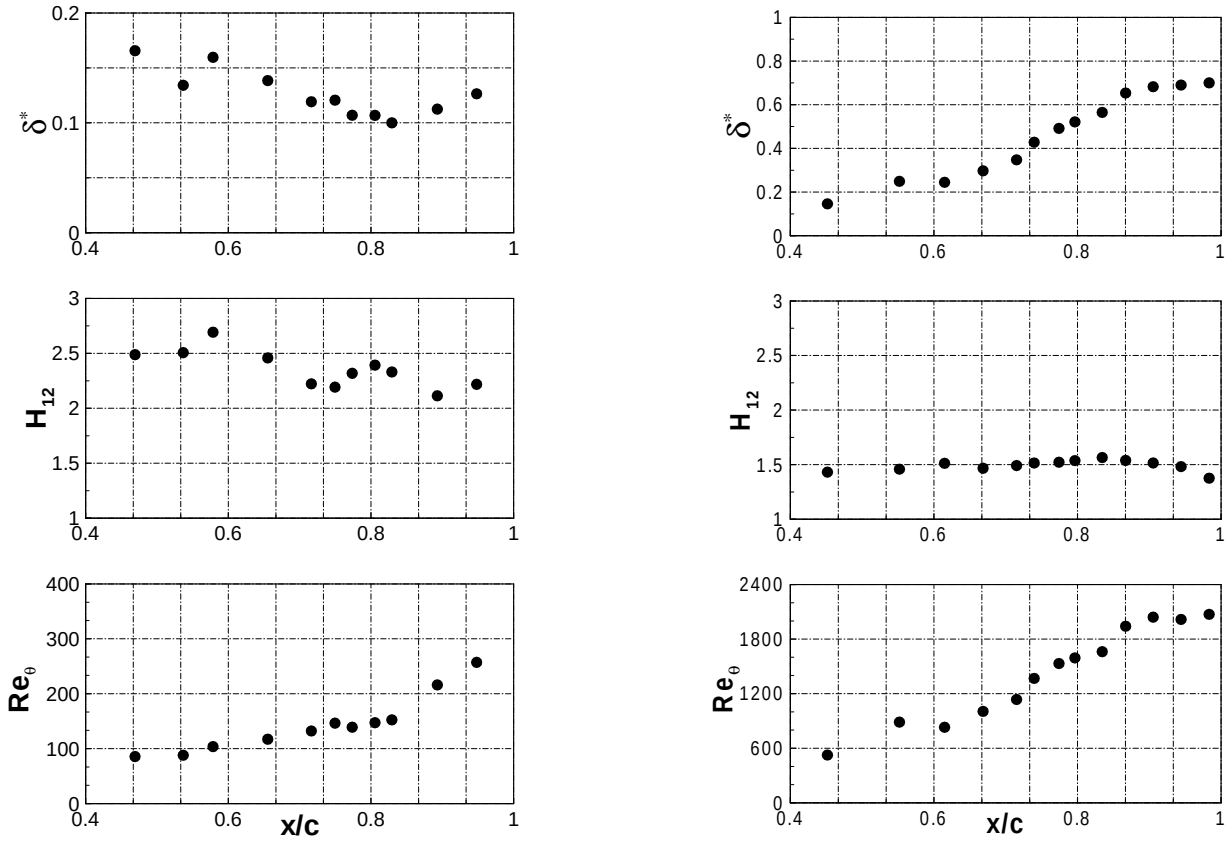

(a) pressure side

(b) suction side

Figure 7: Integral parameters.

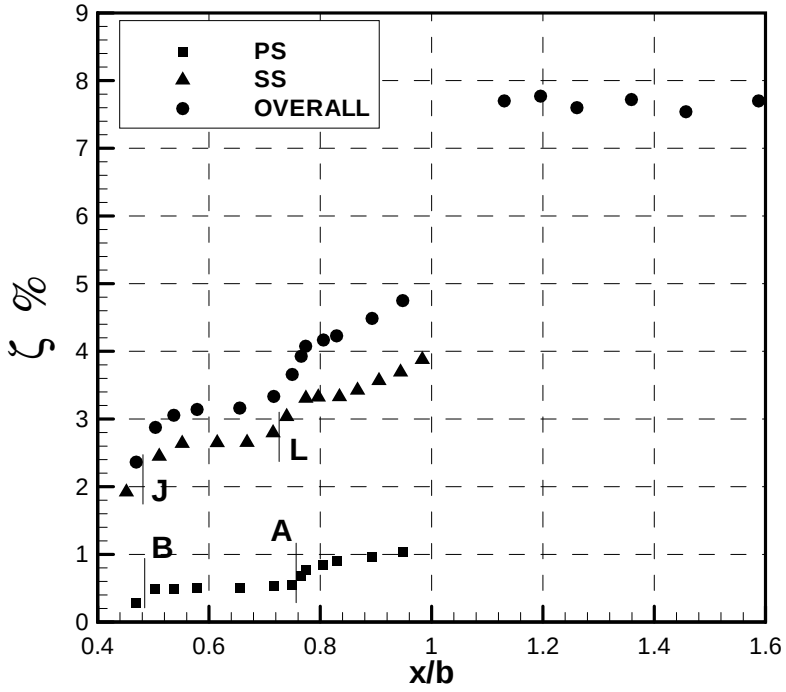

Figure 8: Thermodynamic loss coefficient distribution.

Loss coefficient distribution

LDV boundary layer traverses and downstream 5-hole aerodynamic pressure probe traverses have been used to compute the thermodynamic loss coefficient ζ distribution along both sides of the blade and downstream of the trailing edge presented in Figure 8. These data have been already reported and thoroughly discussed in Barigozzi et al. [7]. It is worth recalling here the definition of the thermodynamic loss coefficient ζ. The 5-hole probe traverses downstream of the cascade allow to compute the following loss coefficient, which includes the losses inside the cooling holes:

$$\zeta = \frac{g_e\left(U_{2,is}^2 - U_2^2\right) + g_c\left(U_{2c,is}^2 - U_2^2\right)}{g_e U_{2,is}^2 + g_c U_{2c,is}^2}$$
$$= 1 - \frac{\left[1+\left(g_c/g_e\right)\right]h_{t2}\left[1-\left(p_2/p_{t2}\right)^{\varphi}\right]}{h_{t1}\left[1-\left(p_2/p_{t1}\right)^{\varphi}\right] + \left(g_c/g_e\right)h_{tc}\left[1-\left(p_2/p_{tc}\right)^{\varphi}\right]}$$

where $\varphi = (\gamma\text{-}1)/\gamma$. Boundary layer traverses (not presented here) allow to evaluate the contribution to the thermodynamic loss, due to the pressure and suction side developing boundary layers, by means of the relation:

$$\zeta = \frac{\int_0^{\delta} \rho u\left(U_e^2 - u^2\right)(1-C)\,dn + \int_0^{\delta} \rho u\left(U_{e,c}^2 - u^2\right)C\,dn}{g_e U_{2,is}^2 + g_c U_{2c,is}^2}$$

where $U_{e,c}$ is the coolant isentropic velocity at the traverse location, resulting from a coolant isentropic expansion from total blade cavity condition to local profile static pressure. This energy loss coefficient has been computed at each boundary layer traverse location, making some assumptions on the coolant concentration C along the traverse. Supposing that all the injected flow

remains inside the boundary layer and assuming an analogy between coolant mass diffusion and momentum diffusion (Osnaghi et al. [12]), the following concentration distribution for the boundary layer traverse at location *s* along the blade surface has been introduced:

$$C(s,n) = \frac{U_e(s) - u(s,n)}{U_e(s)} \; C_{\max}(s)$$

The constant value C_{max} is determined in an iterative way, so that the coolant flow rate, computed by integrating the coolant mass flow rate throughout the boundary layer thickness, equals the coolant mass flow injected along the blade side up to this location.

Figure 8 shows that a quite large loss production takes place across each injection row, followed by a moderate increase up to the next injection row. This behavior could be explained if most of the mixing process takes place very close to injection location. To obtain a deeper insight on these phenomena, a detailed investigation has been performed on the near hole region of the last injection row on both pressure (row A) and suction (row L) side.

The near hole region

Figure 9 (pressure side) and Figure 10 (suction side) present the mean kinetic energy, turbulence intensity and $\overline{u'v'}$ component distributions in eight *(h, n)* planes, starting 1.43 *D* upstream of hole leading edge and reaching approximately 16 *D* downstream. All quantities are normalized with the downstream isentropic velocity U_{2is}. Each contour plot shows a single jet repeated twice. Figure 11 shows the same quantities, but in the *(s, h)* planes closest to the vane surface, located at 0.2 and 0.35 mm from respectively the pressure (row A) and suction (row L) side of the airfoil. Figure 12 presents the same contour plots in the *(s, n)* planes approximately located at hole centerline for both pressure and suction side holes.

Considering the contour plot of Figure 9, in the first measurement plane (*s/D* = -1.43), a quite uniform boundary layer is present, with small *Tu* and $\overline{u'v'}$ values. The presence of the jet issuing from row A can be easily identified in the following plane (*s/D* = 1.43), that is still inside the hole exit region. The jet then assumes the classical “kidney” shape, and in the last plane it seems that the mixing process is nearly completed. Both *Tu* and $\overline{u'v'}$ distributions show that most of the mixing process takes place up to approximately 6*D* downstream of injection location, with maximum *Tu* values of 18 % at *s/D* = 2.86. This is also evident from the contour plots presented in part (a) of Figures 11 and 12. Due to the quite high blowing ratio (*BR* = 1.1), the jet exits the boundary layer. A quite large recirculation area is present right downstream of injection hole, but the strong acceleration push the jet back to the wall. The jets do not merge in spanwise direction.

Less evident are the jets in the suction side case (Figures10, 11 and 12), due to the presence of a thick turbulent boundary layer and coolant injection at low blowing ratio (*BR* = 0.79). The jets remain attached to the wall, as also shown in part (b) of Figures 11 and 12. Also in this case the mixing process seems to take place mostly in the near hole region, up to *s/D* = 6, but of course closest to the wall; it is then approximately completed in the last plane (*s/D* = 15.7) where it results in a strong increase of boundary layer thickness.

CONCLUSION

A comprehensive set of data concerning the 2D flow within a full coverage film cooled airfoil as typical of a nozzle vane of an industrial gas turbine has been presented and discussed. All these experimental data, besides giving a detailed description of near hole coolant jet to main flow mixing process, will be used to validate a novel 3D RANS solver that will be run both for the experimental and the actual gas turbine operating conditions.

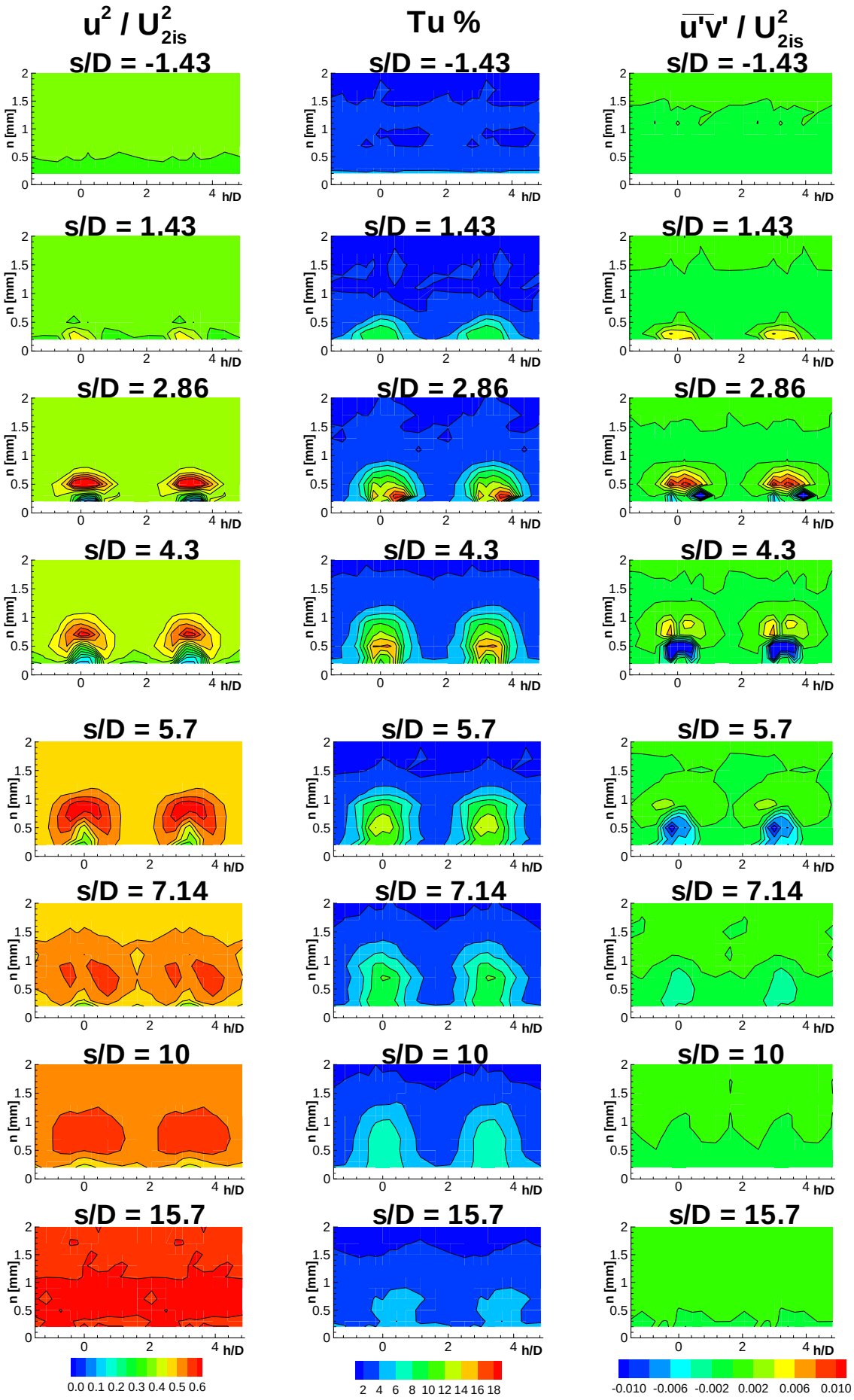

Figure 9: Row A flow distribution (pressure side).

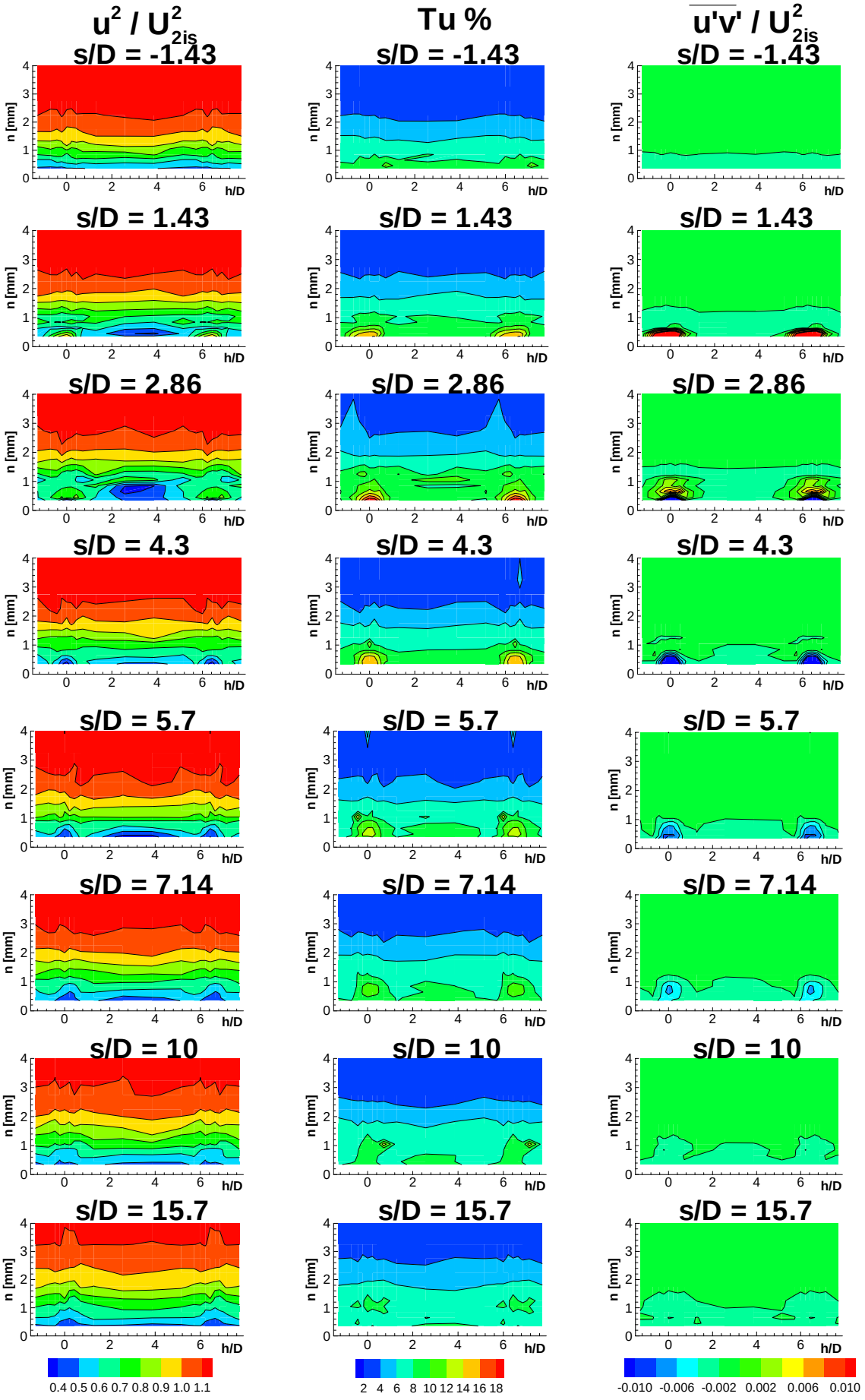

Figure 10: Row L flow distribution (suction side).

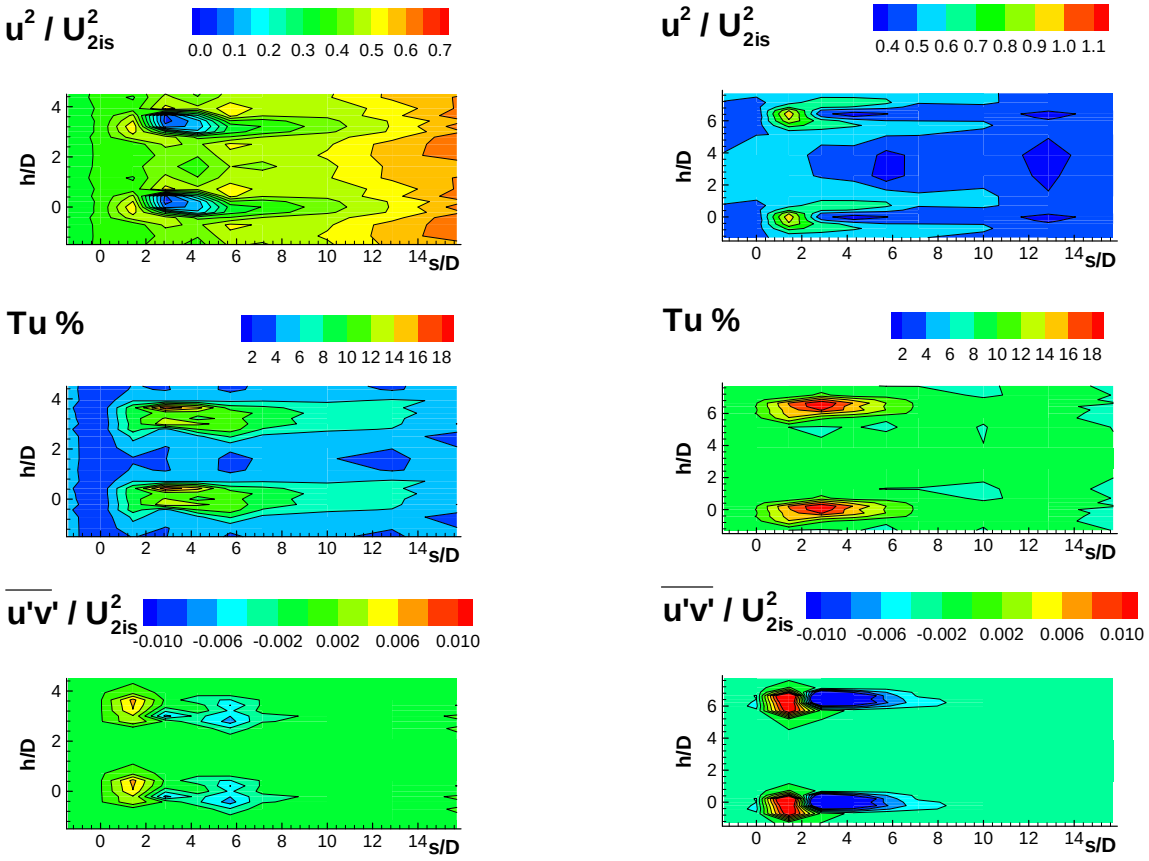

(a) row A (pressure side) (b) row L (suction side)

Figure 11: Flow characteristics in the *s*, *h* plane closest to the wall.

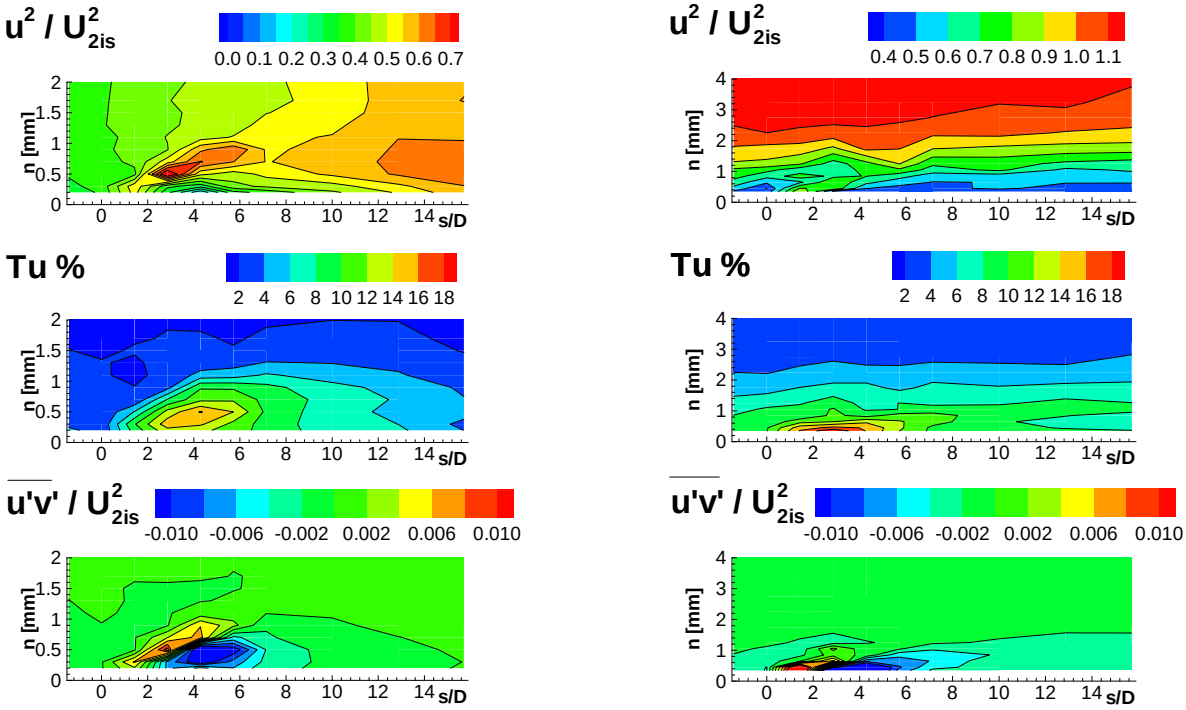

(a) row A (pressure side) (b) row L (suction side)

Figure 12: Hole centerline flow characteristics in the *s*, *n* plane.

REFERENCES

[1] Urban, M.F., Hermeler, J., Hosenfeld, H.-G., 1998, "Experimental and Numerical Investigations of Film-cooling Effects on the Aerodynamic Performance of Transonic Turbine Blades", *ASME Paper 98-GT-546*.

[2] Hartsel, J.E., 1972, "Predictions of Effects of Mass Transfer Cooling on the Blade-Row Efficiency of Turbine Airfoils", *ASME Paper 72-11*.

[3] Walters, D.K., Leylek, J.H., 2000, "Impact of Film-cooling Jets on Turbine Aerodynamic Losses", *ASME Journal of Turbomachinery*, Vol. 122, pp. 537-545.

[4] Bassi, F., Rebay, S., Savini, M., 1998, "Quasi-3D Numerical Computations on a Film-Cooled Gas Turbine Nozzle", *ASME Paper 98-GT-536.*

[5] Ardey, S., Fottner, L., 1998, "A Systematic Experimental Study on the Aerodynamics of Leading Edge Film Cooling on a Large Scale High Pressure Turbine Cascade", *ASME Paper 98-GT-434*.

[6] Brandt, H., Ganzert, W.T., Fottner, L., 2000, "A Presentation of Detailed Experimental Data of a Suction Side Film Cooled Turbine Blade", *ASME Paper 2000-GT-296*.

[7] Barigozzi, G., Benzoni, G., Perdichizzi, A., 2001, "Boundary Layer and Loss Analysis in a Film Cooled Vane", *ASME Paper 2001-GT-0136*, to be presented at the *ASME TURBOEXPO 2001*, New Orleans, USA.

[8] Camci, C., Arts, T., 1990, "An Experimental Convective Heat Transfer Investigation Around a Film-Cooled Gas Turbine Blade", *ASME Journal of Turbomachinery*, Vol.112, pp. 497-503.

[9] Dossena, V., Osnaghi, C., Perdichizzi, A., Savini, M., 1996, "On Testing the Aerodynamics of Film-Cooled Blades", *12th Symposium on Measuring Techniques for Transonic and Supersonic Cascades*, Zurich, September 2-6.

[10] Osnaghi, C., Perdichizzi, A., Savini, M., Harasgama, P., Lutum, E., 1997, "The Influence of Film-Cooling on the Aerodynamic Performance of a Turbine Nozzle Guide Vane", *ASME Paper 97-GT-522*.

[11] Boutier, A., 1991, "Accuracy of Laser Velocimetry", *Lecture Series 1991-05*, VKI, Brussels.

[12] Modarres, D., Tan, H., Nakayama, A., 1988, "Evaluation of Signal Processing Techniques in Laser Anemometry", *4th International Symposium on Application of Laser Anemometry to Fluid Dynamics*, Lisbon.

Paper Number: 30

Name of Discussor: H.B. Weyer, DLR Cologne

Question:
Obviously you use the LDV- anemometry to carry out those impressive mixing test. What size have the particles you used and tried you to seed either the main flow and the coolant flow? Which are the results?

Answer:
Particles dimension has not been really characterised but it's of the order of μm- We seed both coolant and main flow independently .
We investigated the effect of separate cooling and we found that, only very close to injection location, coolant flow seeding is important and this is due to the fact that mixing process is very fast.

Name of Discusser: T. Tinaztepe, Roketsan Turkey

Question:
Is there any effect of secondary flow in your measurement?

Answer:
All measurements have been performed at mid span. Anyway preliminary measurement of secondary flows have shown a large 2 D flow region.